

A Case Study on the Heat Pump Integration for Enhanced Efficiency in Battery-Electric Short-Sea Ferries

Steffen Brötje^{a*}, Markus Mühmer^a, Thorben Schwedt^a,
A. Phong Tran^b and Sören Ehlers^a

^a Institute of Maritime Energy Systems, German Aerospace Center (DLR), 21502 Geesthacht, Germany

^b Institute of Low-Carbon Industrial Processes, German Aerospace Center (DLR), Walther-Pauer-Straße
5, 03046 Cottbus

* Correspondence: steffen.broetje@dlr.de, +49 4152 8488-107

Abstract

This case study investigates the potential of incorporating water heat pumps into onboard thermal systems to utilize low-temperature waste heat for onboard heating and enhance the efficiency and economics of all-electric battery-driven ferries. We analysed a hybrid-driven roll-on/roll-off passenger ferry operating in the Baltic Sea, gathering data on vessel operation, power, and heat provision in low-temperature cycles. We integrated real-time measurement data, energy flow analysis, and thermodynamic calculations to draw conclusions for a potential battery retrofit scenario featuring an all-electric operation and a battery system capacity of 10 MWh. Our results indicate that the integration of heat pumps in battery-electric mode can cover more than 50 % of the onboard nominal heat capacity of HVAC systems, with a seasonal coefficient of performance (SCOP) of 3.5 during the heating season. The overall electric energy demand of the vessel during the 6-month heating period is reduced by approximately 8 % compared with direct-electric heating.

Keywords: Maritime heat pumps, battery-electric ships, low-temperature waste heat, energy efficiency, green maritime technologies

1 INTRODUCTION

The International Maritime Organization (IMO) aims to achieve net-zero GHG emissions from shipping by approximately 2050 [1]. Waterborne transportation produced 3-4 % of the EU's total CO₂ emissions by 2021 [2]. With the "Fit for 55" package and the European Green Deal, the European Commission targets a 55 % GHG reduction by 2030 and climate neutrality by 2050, with shipping emissions included in the EU's emissions trading system [3]. The IPCC highlights efficiency improvements as a key measure for vessels [4]. Legal measures for ship efficiency are the Energy Efficiency Existing Ship Index (EEXI) and the Carbon Intensity Indicator (CII). Integrating water-water heat pumps into heating systems and low-temperature (LT) cooling cycles of all-electric ferries presents a solution for enhancing energy efficiency, thus aligning with these environmental goals.

1.1 Electrification of Short-Sea Ferries

Ferries constitute nearly 10 % of the total commercial value of all types of ships and represent a significant share of the global maritime economy, particularly in Europe, where they conduct the majority of short-sea operations

involving freight and passengers, due to the many islands and archipelagos in the region [3, 5–7].

Historically, electric ships have been smaller, resulting in less complex energy systems. However, the emerging trend of deploying high-capacity batteries in larger short-sea vessels allows the inclusion of more sophisticated energy systems and heat recovery equipment. This shift is evident in the increasing number of commissioned larger electric vessels. Over 2200 Ro-Ro and passenger ferries of 1000 gross tonnage and more are listed in Clarkson's "World Fleet Register" [5].

Harmful emissions from ships, such as SO_x and NO_x, are high, so interventions are needed to meet MARPOL Annex VI amendments and increasingly stringent Emission Control Area (ECA) requirements [6, 8–10].

One promising strategy for reducing these emissions is the electrification of ship energy systems. Battery-electric storage systems (BESS) are becoming increasingly popular, especially for short-range vessels [11]. The number of battery-powered and purely electric vessels in operation and on order is rising, particularly in ferries. The DNV's "Alternative Fuel Insights" database indicates 619 operational battery-powered ships, 158 of which are purely electric. In addition, there are 212 more ships in order, 43 of which are purely

electric. Of the pure electric ships, 115 are ferries, with 33 more in the pipeline [12].

Electric vessels are primarily used in transportation and tourism, with Norway and Denmark leading electrified ferry operations [6, 13]. Two-thirds of electrified vessels operate in a hybrid mode, as battery-electric power is largely dependent on voyage distances [6].

Batteries in hybrid systems help reduce fuel consumption and emissions by allowing for load levelling, peak-shaving, and the potential for temporary engine shutdown [10]. However, deep-sea vessels may not find BESS financially viable because of their high energy needs and long journeys, making carbon-neutral fuels a more appropriate option [11].

Battery electric ships with onshore charging at berths present a significant opportunity to reduce pollutants in ports. Studies have shown potential reductions in fuel costs and emissions of 15–35 % by sourcing power for batteries from onshore grids that utilize renewable energy [8, 10]. Rapidly declining battery prices, now at an average of 100 USD/kWh, and the potential of renewable energy sources, such as wind and solar power, further enhance the viability of this approach [6, 14, 15].

However, the transition to electrification presents challenges like power system optimization and management strategies [10, 14, 16].

Recent advancements in battery systems, characterized by enhanced energy density and reduced weight [17], have facilitated electrification of larger vessels. Consequently, this technological progression has resulted in the elimination of the waste heat originating from combustion engines. Battery-electric vessels have different thermal management systems than diesel or diesel-electric systems because they do not reject high amounts of heat via exhaust gases and cooling water from combustion engines nor do they produce high temperatures (HT).

1.2 Waste Heat Utilization and Heating on Ferries

Diesel and diesel-electric hybrid ships utilize waste heat sourced from engine exhaust or HT cooling water. This heat is applied in various ways depending on the ship type and travel profile, generally through steam coils in fuel tanks and preheaters for different substances, such as fuel oil, lubricating oil, air, and water, along with other technological receivers [18]. On passenger ships, HT waste heat is used for steam generation, direct heating, hot water production, or electricity generation through steam turbines or the Organic Rankine Cycle (ORC). These vessels use waste

heat for hot potable water production and can employ thermal storage to balance the generated and consumed heat [19].

The efficiency of waste heat recovery (WHR) systems is influenced by the temperature of the heat source, making them useful only when there is a corresponding demand. Owing to their customized systems and short distances between heat sources and consumers, ships are suitable for WHR.

Diesel engines running on carbon-neutral fuel are likely to continue to power bulk and container vessels, providing HT heat. Battery-electric ships can operate emission-free with the right renewable power mix, but they only provide low-exergy heat owing to their low cooling circuit temperatures. Heat loss from the propulsion and supply systems of these ships is typically discharged into seawater. Heating systems on board still demand heat at approximately 50 to 70 °C, while drivetrain devices are cooled to a maximum of approximately 40 °C, resulting in a significant energy loss.

The state of the art for heating battery-powered vessels primarily revolves around direct electric heating. In such systems, the electricity from the battery of the vessel is used to directly produce heat through electric heaters with resistive elements. This method is straightforward, simple, and reliable, but not the most energy-efficient [20], especially when compared to heat pumps.

1.3 Heat Pumps in Battery-Electric Ships

Heat pumps are a promising solution for enhancing the energy efficiency of battery-powered electric ships [20]. They can harness the low-temperature waste heat generated by electrical machinery, such as batteries and battery converters [17, 20], to provide heating for passenger ships and other vessels with significant heat and cooling demands. Compared to the benchmark of direct-electric heaters with resistive elements, the use of heat pumps reduces the operational costs of electricity and the required battery capacity. Heat pumps can provide both heating and cooling by reversing the cycle using reversing valves.

However, there are challenges in integrating heat pumps into ships, such as limited space, complexity, upfront costs, and the need to be installed near the heat source [21]. The speed of response of water heat pump systems also tends to be slower than with local direct-electric heating. A secondary heat source must be implemented to provide heat during low operation losses and high heat demands. Additionally, the refrigerants used in some heat pumps can have environmental implications if not properly managed.

The feasibility of heat pump integration is closely related to vessel size and heating requirements. Electric cabling is typically less expensive than fluid piping. As equipment costs do not scale linearly with size and electricity costs for heating are nearly proportional to power demand, the increasing size of ships and electric capacities favour the potential of utilising low-temperature waste heat, particularly on ferries with significant heat demand.

We assessed the use of water-water heat pumps to recover this waste heat in BESS-equipped all-electric ships, such as RoPax ferries. This can reduce energy use, emissions, and battery load for direct-electric heating. The upscaling of electric systems leads to an increase in LT waste heat, specifically originating from batteries and battery converters for the grid and consumers. This waste heat can be repurposed for onboard heating using specially designed heat pump systems.

To validate this, we investigate the integration of a heat pump system into a Baltic Sea ferry, recording heat and energy flows, and simulating the potential energy savings following a hypothetical conversion to a fully electric ferry.

2 HEAT FLOW ANALYSIS

2.1 Hybrid-electric ferry specifications

A measurement campaign was conducted on the hybrid-electric RoPax ferry "Schleswig-Holstein" over five days in November and December 2022 to assess the feasibility of using heat pumps for a potential retrofit to all-electric operation. This study does not evaluate the conversion itself but instead develops a theoretical model scenario for a possible system layout. Figure 1 shows the ferry in operation.



Figure 1: Hybrid-electric ferry "Schleswig-Holstein" (Source: Scandlines)

Table 1 presents the system. The ferry is powered by a 2,600-kWh NMC battery system and up to four diesel generators, ranging from 2,640 kW to 4,950 kW. The Corvus battery system provides low-speed propulsion, load balancing, and power for onboard operation. In normal operation, load levelling is achieved by running the 9-cylinder engine and the battery system, charging

the ESS during port time, and discharging it during cruising. The 6-cylinder engine was used only once during the measurement period because of a scrubber system refill requirement. Diesel generators ensure safe manoeuvrability and compliance with the SOLAS regulations. Figure 2 shows all completed voyages between Puttgarden, Germany and Rødbyhavn, Denmark, undertaken during the measurement campaign.

Table 1: Specifications of investigated hybrid-electric ferry

Basic Specifications	
Length	142.0 m
Width	24.4 m
Gross tonnage	15,187 GT
Gross deadweight	2,904 t
Operational speed	18.5 kn
Machinery & Propulsion	
GenSet, MAK 9M32E + 3 Ph 50 Hz 6600 V/245 A	1 x 4,950 kW
GenSet, MAK 8M32 + 3 Ph 50 Hz 6600 V/330 A	2 x 3,520 kW
GenSet, MAK 6M32 + 3 Ph 50 Hz 6600 V/519 A	1 x 2,640 kW
ESS, Corvus	2,600 kWh 3,500 kW
Kongsberg Azimuth Thruster AZP 120 FP	4x 3,000 kW

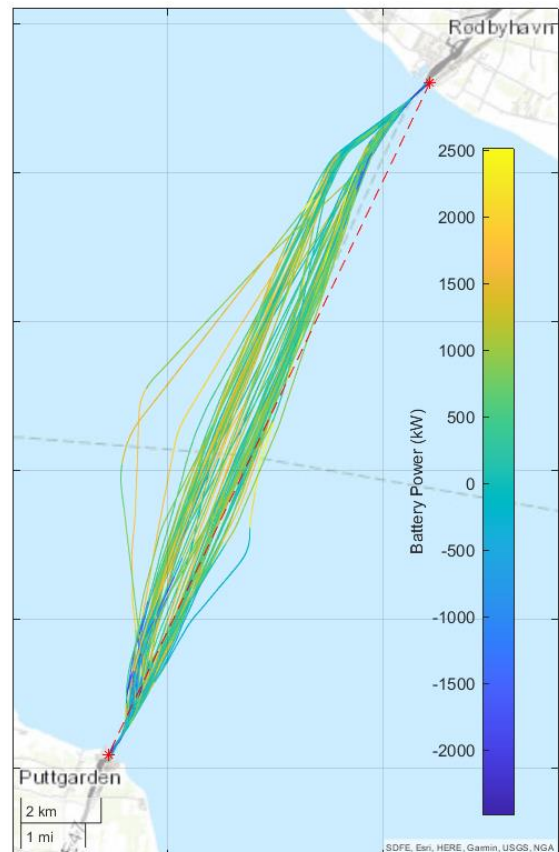


Figure 2: Voyage routes during measurements

2.2 Data acquisition

Measurements were collected from the NMEA interface, the monitoring and surveillance system in the engine control room, and via heat flow measurements on the low-temperature cooling circuit.

2.2.1 Navigational and power data

A custom Raspberry Pi data-logger, attached to the NMEA 0183 interface near the northern bridge, recorded time-dependent propulsion power, power consumption, navigation, and position data. Managed by the National Marine Electronics Association, NMEA 0183 enables communication between marine electronics. The text-based output was synchronized with the heat flow measurements and correlated with the ship operations. Figure 3 depicts the repeated route of the hybrid ferry during the main measurement activities, as indicated by the latitude position, along with the total energy consumption of each round trip. The repetitiveness of the cycle simplifies the measurement and modelling owing to the constant boundary conditions. The seawater and ambient air temperatures are also illustrated.

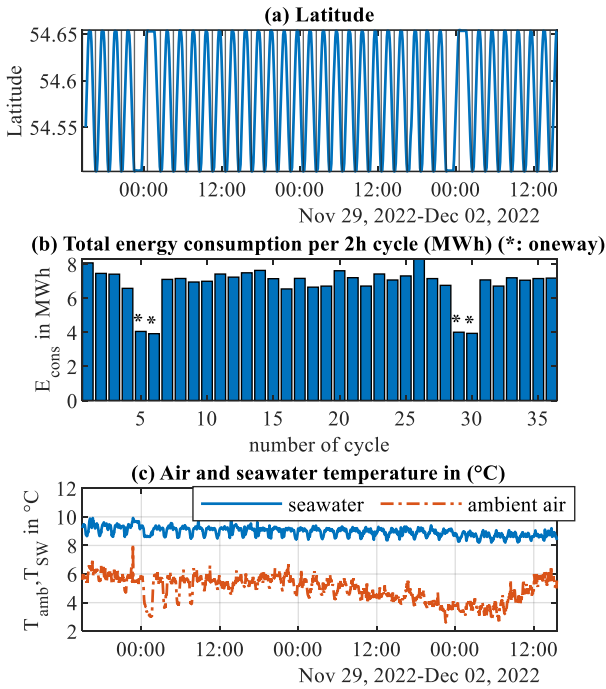


Figure 3: Round trips acc. to NMEA data:

- (a) Latitude of ship in 2-hour cycles (Puttgarden-Rødbyhavn-Puttgarden)
- (b) Total energy consumption per round trip (*: only one-way trip Putt.-Rødby./Rødby.-Putt.)
- (c) Air and seawater temperature

2.2.2 Heat flow rate measurements

Four portable dual-channel ultrasonic flow meters were used to measure the heat flow rates in the LT cooling system of the hybrid-electric ferry,

covering heat-rejecting components such as converters, ESS, and electric motors. Additionally, Surplus heat from the 9-cylinder diesel and 160 °C thermal recovery system was tracked for heat balance evaluation after electrification. Some electric drivetrain parts, such as transformers, are dry-cooled and not part the LT system. Ultrasonic sensors were clamped at either the inlet or outlet of the cooling cycle to acquire the volume flow rates \dot{V}_i . The inlet and outlet temperatures T_1 and T_2 were measured using resistance thermometers of type Pt100. We used Eq. (1) to determine the enthalpy flow difference between two points in the cooling system, noting that the fluid properties of water, such as density $\rho(\bar{T})$ and specific heat $c_p(\bar{T})$, remain relatively stable with temperature.

$$\dot{Q}_i = \dot{m} \Delta H = \dot{V}_i \rho(\bar{T}) c_p(\bar{T}) (T_2 - T_1) \quad (1)$$



Figure 4: Setup of heat flow rate measurement from cooling of the battery's bidirectional converter

The heat flow rates rejected by each component are presented in Table 2. The primary LT cooling ranged between 26 and 30 °C, while the return was 30 to 35 °C before seawater cooling.

In addition to the listed points, enthalpy differences at key cooling system branches were measured but disregarded due to minimal temperature differences and the resulting high enthalpy rate uncertainties.

Figure 4 shows an exemplary measurement setup: the flow meter is at the bottom, temperature sensors T1 and T2 are at the inlet and outlet, respectively, and both the sending and receiving ultrasonic sensors are on the outlet pipe.

2.3 Measurement results

The power data and LT heat flow rates for the ship are listed in Table 3, with the overall mean weighted by the duration of each test.

Approximately 87 % of the LT heat originates from the diesel genset. Figure 5 displays the power rates in the hybrid-electric system and a comparison of overall LT heat transferred to seawater with the LT cooling waste heat of the diesel-generator during an exemplary set of measurements. Deducting the LT heat of the diesel

genset and the HT surplus from the total LT heat rejected to seawater provides an estimate for potential battery-powered ships (Eq. 2).

$$\dot{Q}_{\text{Test}} = |\dot{Q}_{\text{SW}}| - \dot{Q}_{\text{DG}} - \dot{Q}_{\text{SP}} = 272 \text{ kW} \quad (2)$$

The uncertainty of the estimation was high owing to the fluctuation in the highest heat flow rates. Therefore, the potential LT heat available in the all-electric scenario is calculated by summing all the heat rejected by the electric drive system units, as shown in Eq. (3).

Table 2: Water-cooled heat sources and parameters in low-temperature cooling cycle

Location/unit	Type (cooling details)	Rated power per unit (kW)	Rated losses per unit (kW)	Diameter (ND)	Rated water flow rate (m ³ /h)
Battery ESS	NMC Li-Ion (3-Stage compressor + water-air HEX)	3,500	60	50	11.9
ESS converter	Bidirectional (water-cooled)	4,000	40	60	5.3
Thruster Motor (4x) ^a	3-Phase (air-cooled, air-water HEX)	3,100	126	50	15.5
Azimuth Thruster	(valves closed during measurements)	3,000	150	65	21
Thruster frequency converter (4x) ^b	24 Pulse DFE Rectifier + Inverter	3,100	61	50	12.5
Provisions cooler	(provisions partially water-cooled)	16	16	50	3
HT Surplus ^c	Plate HEX (from 160 °C-system)	250	250	50	25
Diesel Genset 5 ^c (LT cycle only)	4-stroke recipro. piston inline engine + 3-Phase 50 Hz generator	4,950	3,500	100	93
Seawater HEX	Plate HEX	/	-11,098	300	342.0

^a 4 Azipull Thrusters; heat flow rate at No. 2 and 4 was measured; losses for No. 1 and 3 assumed to be the same

^b Heat flow rates of No. 1 and 2 were measured, losses for No. 3 and 4 assumed to be the same

^c Diesel engines and HT surplus obsolete in all-electric scenario; DG 5 was only genset running during evaluation

Table 3: Measured power and heat flow rates

Location/unit	Name	Dimension	Source	Min.	Max	Weighted average
Power						
Diesel Generator 5	P_{DG5}	MW _{el}	NMEA	- ^a	- ^a	3.63
Battery Power	P_{ESS}	MW _{el}	NMEA	-2.39	2.12	-0.07
Consumption (total)	P_{Con}	MW _{el}	NMEA	0.22	6.61	3.56
Thrusters (sum)	P_{Thr}	MW _{el}	NMEA	0.00	4.66	2.18
Thermal system						
Seawater heat exchanger	\dot{Q}_{SW}	kW _{th}	HFM	-3,356	329	-2,087
Diesel Genset 5 (LT heat rejected)	\dot{Q}_{DG}	kW _{th}	HFM	-511	2,173	1,816
HT System (Surplus from 160°C-system)	\dot{Q}_{SP}	kW _{th}	HFM	2	19	11
Heat to seawater (excl. \dot{Q}_{DG} , \dot{Q}_{SP})	\dot{Q}_{Test}	kW _{th}	HFM	-	-	272
Heat rejected by electric drive system units						
Battery ESS	\dot{Q}_{ESS}	kW _{th}	HFM	8	90	32
Battery ESS converter	\dot{Q}_{EC}	kW _{th}	HFM	1	20	9
Thruster Motor No. 2 & 4	$\dot{Q}_{\text{Th2/4}}$	kW _{th}	HFM	6 / 3	37 / 32	23 / 21
Thruster frequency converter No. 1 & 2	$\dot{Q}_{\text{TC1/2}}$	kW _{th}	HFM	7 / 9	38 / 43	20 / 24
Provisions cooler ^b	\dot{Q}_{Pr}	kW _{th}	HFM		10	10

^a Generator Power calculated indirectly from total power output and battery power. Min/Max values not reliable due to low frequency of battery power signal; ^b Assumption

NMEA: data achieved from NMEA Interface signals and own calculations

HFM: data achieved from heat flow rate measurements and own calculations

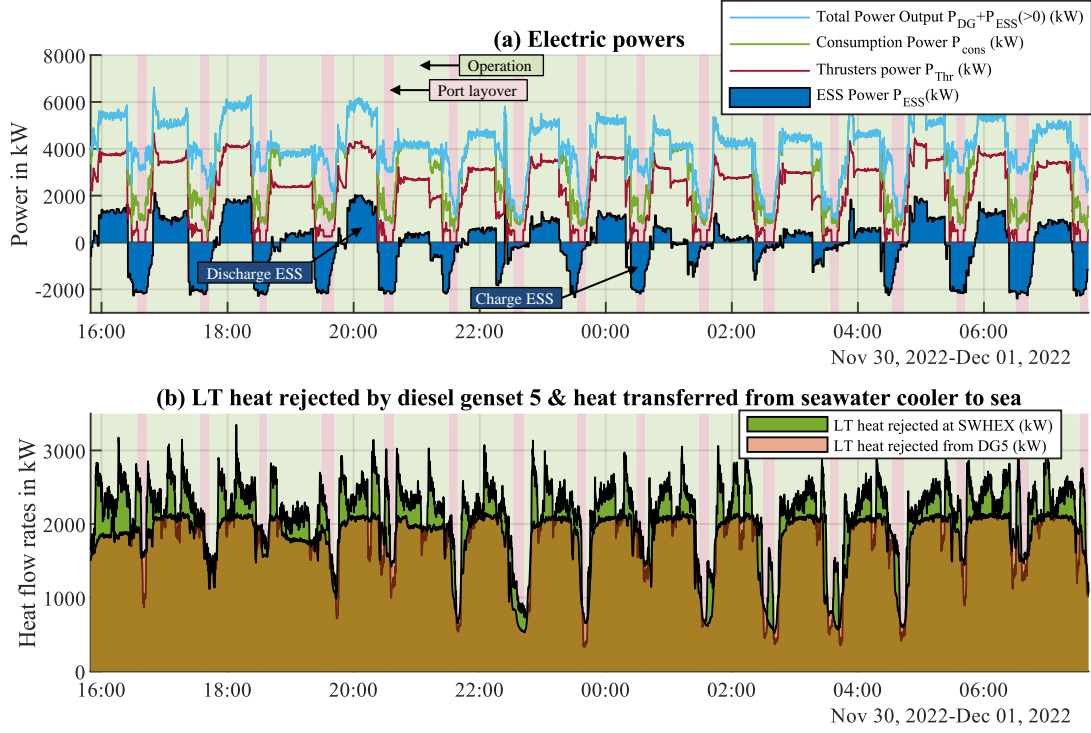


Figure 5: Exemplary signal plots

- (a) Power rates of battery, consumers (propulsion + hotel), propulsion and total output
(b) LT heat flow rates at seawater heat exchanger and main engine 5

$$\begin{aligned} \dot{Q}_{LT,el} = \dot{Q}_{ESS} + \dot{Q}_{EC} + 2 \dot{Q}_{Th2} + 2 \dot{Q}_{Th4} \\ + 2 \dot{Q}_{TC1} + 2 \dot{Q}_{TC2} + \dot{Q}_{Pr} = 227 \text{ kW} \end{aligned} \quad (3)$$

The 227 kW value represents the minimal LT heat in colder seasons for the present ship setup, excluding the fuel heat sources. The disparity between \dot{Q}_{Test} and $\dot{Q}_{LT,el}$ indicates significant uncertainties in the major heat sources and heat transfer to the sea. In addition, the system also includes three more diesel engines in standby, contributing heat via a complex cooling and fuel preheating system of non-insulated HT parts next to the LT cooling pipes.

Notably, each thruster motor and its grid converter have approximately 4 % loss relative to the power of each thruster. 227 kW signifies a roughly 6 % loss in total consumption. In a fully electric battery-operated mode, crucial electric drivetrain elements, such as the battery system and converter, will increase, adding more LT heat for heat pumps. Moreover, more electric consumers are expected in all-electric vessels, including the heat pump system. This is further explained in Section 3.

3 ALL-ELECTRIC SCENARIO

The transition to fully electric operation poses a challenge considering that the Rødby-Puttgarden route covers 18.5 km, and the current schedule only allows for a 15-minute layover at each port for quick charging [22].

This chapter employs a basic voyage and charging profile to project LT heat availability in a hypothetical all-electric ferry. This scenario is unconfirmed, and decisions for such large retrofit and grid projects must consider factors beyond efficiency.

3.1 Battery losses

Heat losses from the upscaled battery system during charging, discharging, and pausing are accounted for and estimated through a basic correlation to power. [23]:

$$\dot{Q}_{ESS} = k P_{ESS}^2 \quad (4)$$

The loss factor k is defined as equal for both the charging and discharging processes. High losses diminish the benefits of high charging rates and accelerate battery cell aging. The actual power and heat losses of a battery system depend on cell type, cell size, cooling system, and topology. Losses have been described in several studies for different cell types such as LMO, NMC, LTO, and LFP. [15, 24–26]. MAN Energy Solutions observed that while charging a 1 MWh battery at a C-rate of 3, there is a heat loss power ranging from 4 % to 6 %. As the C-rate increases, the heat loss also increases [27]. A loss of 5 % at a C-rate of 3 is assumed for the following scenarios, resulting in $k = 1.67e-6$.

3.2 All-electric voyage profile

Switching to an all-electric system implies replacing diesel engines with larger battery systems. A scenario was created to assess how altered charging strategies and battery losses affect the heat released to the low-temperature cycle and its usability for heat pumps.

Table 4 details this scenario. A 10 MWh battery system is charged at both ports using 15 MW onshore power, indicating a 1.5 C-Rate as a near-future solution. To maintain manoeuvrability and energy levels, a 17-minute charge at each port with a 41 % DoD is needed.

Table 4: Modelled all-electric scenario in comparison to existing hybrid-electric operation

	Hybrid	All-electric
Route time and power profile		
Charging time per port t_{chg} (Min.)	-	17
Cruise time t_{op} (Min.)	45	45
Pause time in port t_{pause} (Min.)	15	3
One-way voyage time (Min.)	60	65
C-Rate (port charge)	-	1.5
Propulsion (cruise) P_{Thr} (kW)	2,907	2,907
Hotel loads P_{hotel} (kW)	1,380	1,780
Consumption (cruise) P_{op} (kW)	4,287	4,687
Consumption (mean) (kW)	3,560	3,792
Overall genset capacity (kW)	14,430	-
ESS capacity (kWh)	2,600	10,000
ESS power capacity (kW)	3,500	15,000
Energy balance		
Charging power P_{chg} (kW)	(919)	15,000
C-Rate charge	(0.35)	1.5
Losses charging ϵ_{chg} (%)	-	2.5
Cruise power P_{op} (kW)	(760)	4,687
C-Rate discharge	(0.29)	0.47
Losses discharge ϵ_{op} (%)	-	0.8
C-Rate hotel mode	(0.53)	0.18
Losses pause ϵ_{pause} (%)	-	0.3
Charged energy E_{chg} (kWh, excl. losses)		4,144
Required energy E_{req} (kWh, incl. losses)		4,138

The mean hotel load for the hybrid ship was 1382 kW. Further 200 kW are assumed for the heat pump consumption and 200 kW for new electric consumers expected on the all-electric ship. Thus, 1782 kW is considered a constant hotel load.

The charging and discharging losses are considered in the energy balance, according to Eq. (4). The scenario is set up to be potentially operated fully electric, as there is more energy charged than consumed due to losses. The charged and required energies for a one-way voyage (half-round trip) were calculated using Eq. (5) and (6), assuming

that the EMS allows for the simultaneous charging and provision of hotel loads:

$$E_{\text{chg}} = P_{\text{chg}} \frac{t_{\text{chg}}}{60 \text{ Min/h}} \cdot (1 - \epsilon_{\text{chg}}) \quad (5)$$

$$E_{\text{req}} = \frac{P_{\text{op}}}{(1 - \epsilon_{\text{op}})} \frac{t_{\text{op}}}{60 \text{ Min/h}} + \frac{P_{\text{hotel}}}{(1 - \epsilon_{\text{hotel}})} \frac{t_{\text{chg}} + t_{\text{pause}}}{60 \text{ Min/h}} \quad (6)$$

The change in the operation profile and battery upscaling from 2.6 to 10 MWh affect parts of the LT cooling cycle, particularly the battery cooling heat rates at the battery chiller and battery converter. The total LT heat rates available for the heat pump are listed in Table 5.

The battery chiller heat rates are acquired from the battery losses, as shown in Eq. (4) and Table 4, assuming heat transfer of the losses to the cooling water with 90 % efficiency. The presented heat flow rates are the mean values of all times of the standard route schedule, including cruise, charging, and additional port times. To assess the potential of heat pump applications, the mean values are considered sufficient because of the unresponsive slow behaviour of the thermal system.

In the all-electric mode, there is 346 kW of heat available at low-temperatures of approximately 30 °C. Excluding the diesel-genset losses, this is an increase of 50 % compared with the hybrid system.

Table 5: Available LT heat rates in all-electric mode

	Hybrid	All-electric
Heat rejected to LT cooling water system (kW)		
ESS (charge)	-	375
ESS (operation)	-	36.6
ESS (pause)	-	5.3
ESS (mean)	32	124 x 0.9
ESS Converter	9	39
Constant values (measured kW, see Table 3)		
Thruster Motor 2	2 x 23	
Thruster Motor 4	2 x 21	
Thr. frequency converter 1	2 x 20	
Thr. frequency converter 2	2 x 24	
Proviand	2 x 10	
Sum $\dot{Q}_{\text{LT,av}}$ (kW)	227	→ 346

4 HEAT PUMP INTEGRATION

4.1 Heat pump model

To assess the performance of the proposed heat pump, a parametric study was conducted using a simulation model implemented in the Modelica Buildings library [28]. A constant second-law efficiency, denoted as η , is assumed for the heat pump, which relates the heat pump's coefficient of performance (COP) to the Carnot cycle COP using Eq. (7):

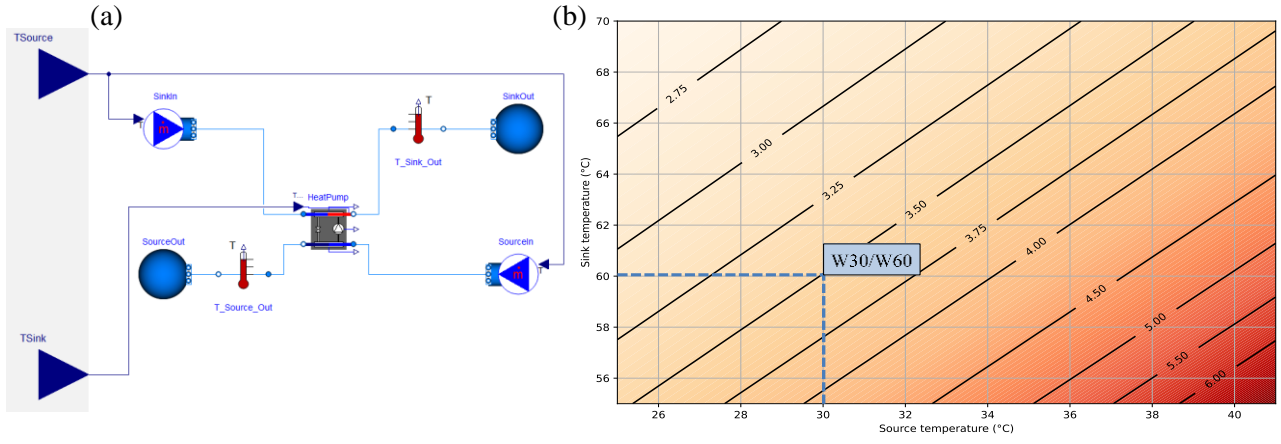


Figure 6: (a) Modelica-based model for presented heat pump study
(b) Coefficient of performance (COP) of the heat pump at various source and sink temperatures.

$$\text{COP} = \eta \cdot \text{COP}_{\text{Carnot}} \quad (7)$$

$$\text{where } \text{COP}_{\text{Carnot}} = \frac{T_h}{T_h - T_l}$$

Arpagaus et al. [29] compiled the performance data of commercially available industrial heat pumps and reported Carnot efficiencies of 40 % to 60 % for most heat pumps. For this study, a Carnot efficiency of 50 % was assumed. Moreover, a terminal temperature difference of 2 K was considered for both the evaporator and condenser. The heat source temperature was varied between 25 and 41 °C, whereas the heat sink temperatures ranged between 55 and 70 °C. See the next section for a description of the chosen temperature ranges.

Figure 6 illustrates the COP of the proposed heat pump as a function of the source and sink temperatures as well as the system model used.

4.2 Estimation of energy savings

To estimate energy savings, a water-water heat pump with source/sink temperatures of 30 °C/60 °C (W30/W60) was considered. The ship could consistently maintain the 30 °C source. The system's design caps at 41 °C to safeguard equipment like lithium-ion batteries, from thermal runaway. Although the hybrid ferry's heating system is designed for 65 °C to 70 °C, the considered HVAC systems can effectively operate at 55 °C to 60 °C.

With a COP of 3.5, the heat pump generates 3.5 times the heat for each kWh of electricity. Its energy demand is substantially lower than that of the direct-electric heaters. The energy savings for a 6-month heating period were estimated.

Table 6 illustrates the energy savings for the W30/W60 mode heat pump with a 3.5 seasonal coefficient of performance (SCOP). Used for the HVAC registers, the heat pump can supply 50 % of the peak design heat rate of the system. Because heating systems are typically designed for very

cold winter days, the pump is expected to offer substantial heat, reducing the need for direct electric heating. This will be investigated in a future study.

The heat pump can substantially meet onboard heating needs, saving up to 0.5 million euros annually, depending on electricity costs. While decentralized renewables might cost less than 0.30 €/kWh, grid costs often increase the price.

Using only electric heaters instead of a heat pump for the heating of the ship means drawing all the energy from the ESS. The hotel load increased correspondingly to 2126 kW. Using Eq. (6), the required energy E_{req} per half-round trip would increase from 4138 to 4518 kWh, adding approximately 2 min of port-charging time. Correspondingly, the heat pump can cut energy requirements by approximately 8.4 % and decrease the battery capacity requirements by 380 kWh.

Table 6: Estimations of energy and cost savings, compared to 100 % electric heaters

	All-electric mode
Heat available at ca. 30 °C $\dot{Q}_{\text{LT,av}}$	346 kW _{th}
COP at W30/W60	3.5
Heat pump power demand	138 kW _{el}
Heat available at 60 °C*	484 kW_{th}
Assumed electricity price	0.30 €/kWh _{el}
Days of heating period	182.5 days
Financial saving per year	454,000 €
Savings of energy per round trip	8.4 %
Potential savings of ESS capacity	380 kWh
*Comparison: fraction of maximum (rated) heat for	
... HVAC (898 kW)	54 %
... Radiators (535 kW)	91 %

5 CONCLUSION

This study analysed the possible use of heat pumps in battery-electric ferries, particularly

considering retrofitting a hybrid-electric RoPax ferry. The main findings are as follows:

The ferry cooling system allows substantial heat recovery for onboard air-conditioning. In a fully electric system, the available low-temperature heat for heat pumps increases by 50 % compared to the existing hybrid setup.

Using a Modelica-based model, a heat pump was studied parametrically. With a Carnot efficiency of 50 %, the Coefficient of Performance (COP) of the heat pump was found to be significantly influenced by the source and sink temperatures. Notably, a COP of 3.5 was determined to be very likely for the heat pump, indicating its efficiency in energy conversion.

Integrating heat pumps into the heating system results in an 8 % reduction in the vessel's electric energy demand over a 6-month heating period compared to a benchmark of direct-electric heating with resistive elements. This reduction not only optimizes the energy consumption but also positively impacts the required battery capacity. For a 15,187 GT vessel, the potential annual savings approach 0.5 million euros, although these savings are highly sensitive to shore energy prices.

The operational and charging profiles of the ferry significantly influence the efficiency of an all-electric system. Although hypothetical, the model scenario highlights challenges in transitioning to fully electric operation. The integration of heat pumps into battery-electric ferries presents an energy-efficient and economically viable solution. This study offers guidance for future maritime retrofitting and sustainable operational decisions.

6 OUTLOOK

Heat pump integration necessitates a comprehensive design that links the onboard systems [30, 31]. Adaptation methods for retrofits can be sourced from sectors, such as buildings [32]. The design variables include the specific heating demand and cooling heat of battery systems and power electronics, which can fluctuate owing to elements such as cell size, cooling system, topology, and cell type [15, 24–26].

Future research should consider the dynamics of heat receivers and sources, influenced by passenger numbers, boundary conditions, operation schedules, and the impact of different route scenarios. Specific heat demand profiles will be the subject of future research.

Seasonal effects, especially cooling needs during the summer months, require further exploration of bidirectional heat pump usage. Exploring thermal storage for balancing heat production and demand and utilizing sustainable

working fluids, such as CO₂ and NH₃ in heat pumps is aligned with sustainability objectives.

Demonstrators and system models provide invaluable performance data for optimizing these technologies. As highlighted in section 1.3, vessel size is essential in assessing the feasibility of heat pump integration, necessitating an analysis comparing upfront costs to potential savings.

APPENDIX

A.1 Nomenclature

ε	Losses	%
ρ	Density	kg/m ³
η	Second-law efficiency	-
c_p	Specific heat capacity	J/(kg K)
E	Energy	kWh
ΔH	Enthalpy difference	kJ/kg
k	Battery loss factor	√kW
\dot{m}	Water mass flow	kg/s
P_i	Electric power (of part i)	MW
\dot{Q}_i	Rejected heat flow rate (of part i)	kW
t_i	Time interval	Min.
$T_{1/2}$	Temperature inlet / outlet	°C
T_h	Temperature of hot reservoir	K
T_l	Temperature of cold reservoir	K
\dot{V}_i	Volume flow rate	m ³ /s

A.2 Abbreviations

COP	Coefficient of Performance
DoD	Depth of discharge
EMS	Energy Management System
HEX	Heat exchanger
HT	High-temperature
HVAC	Heating, Ventilation and Air Conditioning
LT	Low-temperature
Ro-Ro	Roll-on/roll-off
RoPax	Roll-on/roll-off passenger vessel
SCOP	Seasonal coeff. of performance
SW	Seawater

REFERENCES

- [1] IMO. "Revised GHG reduction strategy for global shipping adopted." <https://www.imo.org/en/MediaCentre/PressBriefings/pages/Revised-GHG-reduction-strategy-for-global-shipping-adopted-.aspx> (accessed Jul. 8, 2023).
- [2] European Commission. "European Green Deal: Agreement reached on cutting maritime transport emissions by promoting sustainable fuels for shipping." https://ec.europa.eu/commission/presscorner/detail/en/ip_23_1813 (accessed Jul. 8, 2023).
- [3] United Nations Conference on Trade and Development (UNCTAD), Navigating stormy waters, Review of maritime transport. Geneva, vol. 2022.

- [4] M. Pathak, R. Slade, P. R. Shukla, J. Skea, R. Pichs-Madruga, and D. Üрге-Vorsatz, "Technical Summary. In: Climate Change 2022: Mitigation of Climate Change. Contribution of Working Group III to the Sixth Assessment Report of the IPCC," IPCC, Cambridge and New York, 2022.
- [5] Clarkson Research. "World Fleet Register." www.clarksons.net (accessed Apr. 21, 2023).
- [6] S. Anwar, M. Y. I. Zia, M. Rashid, G. Z. de Rubens, and P. Enevoldsen, "Towards Ferry Electrification in the Maritime Sector," *Energies*, vol. 13, no. 24, p. 6506, 2020, doi: 10.3390/en13246506.
- [7] M. Brambilla and A. Martino, *The EU maritime transport system Focus on ferries: Research for Tran Committee*. Brussels: European Parliament, doi: 10.2861/657769.
- [8] H. Winnes, L. Styhre, and E. Fridell, "Reducing GHG emissions from ships in port areas," *Research in Transportation Business & Management*, vol. 17, pp. 73–82, 2015, doi: 10.1016/j.rtbm.2015.10.008.
- [9] A. Torvanger, J. Tvedt, and I. B. Hovi, "Carbon dioxide mitigation from public procurement with environmental conditions: The case of short-sea shipping in Norway," *Maritime Transport Research*, vol. 4, p. 100085, 2023, doi: 10.1016/j.martra.2023.100085.
- [10] H. P. Nguyen et al., "The electric propulsion system as a green solution for management strategy of CO₂ emission in ocean shipping: A comprehensive review," *Int Trans Electr Energy Syst*, vol. 31, no. 11, 2021, doi: 10.1002/2050-7038.12580.
- [11] M. Kolodziejski and I. Michalska-Pozoga, "Battery Energy Storage Systems in Ships' Hybrid/Electric Propulsion Systems," *Energies*, vol. 16, no. 3, p. 1122, 2023, doi: 10.3390/en16031122.
- [12] DNV. "DNV "Alternative Fuels Insight" Database." <https://afi.dnv.com/statistics/> (accessed May. 22, 2023).
- [13] S. R. Sæther and E. Moe, "A green maritime shift: Lessons from the electrification of ferries in Norway," *Energy Research & Social Science*, vol. 81, p. 102282, 2021, doi: 10.1016/j.erss.2021.102282.
- [14] S. Wen et al., "Coordinated Optimal Energy Management and Voyage Scheduling for All-Electric Ships Based on Predicted Shore-Side Electricity Price," *IEEE Trans. on Ind. Applicat.*, vol. 57, no. 1, pp. 139–148, 2021, doi: 10.1109/TIA.2020.3034290.
- [15] J. Kersey, N. D. Popovich, and A. A. Phadke, "Rapid battery cost declines accelerate the prospects of all-electric interregional container shipping," *Nat Energy*, vol. 7, no. 7, pp. 664–674, 2022, doi: 10.1038/s41560-022-01065-y.
- [16] V. M. Moreno and A. Pigazo, "Future Trends in Electric Propulsion Systems for Commercial Vessels," *Journal of Maritime Research*, Vol. IV. No. 2, pp. 81–100, 2007.
- [17] J. Verma and D. Kumar, "Recent developments in energy storage systems for marine environment," *Mater. Adv.*, vol. 2, no. 21, pp. 6800–6815, 2021, doi: 10.1039/D1MA00746G.
- [18] D. Bocheński and D. Kreft, "Cargo Ships' Heat Demand - Operational Experiment," *Polish Maritime Research*, vol. 27, no. 4, pp. 60–66, 2020, doi: 10.2478/pomr-2020-0066.
- [19] M. Manzan et al., "Potential of thermal storage for hot potable water distribution in cruise ships," *Energy Procedia*, vol. 148, pp. 1105–1112, 2018, doi: 10.1016/j.egypro.2018.08.044.
- [20] S. Trzebiński, "Technical Aspects of Using the Heat Pump at the Ship," *Scientific Journal of Polish Naval Academy*, vol. 217, no. 2, pp. 5–15, 2019, doi: 10.2478/sjpna-2019-0009.
- [21] A. Brækken, C. Gabriellii, and N. Nord, "Energy use and energy efficiency in cruise ship hotel systems in a Nordic climate," *Energy Conversion and Management*, vol. 288, p. 117121, 2023, doi: 10.1016/j.enconman.2023.117121.
- [22] Scandlines Deutschland GmbH. "Zero emission freight ferry." <https://www.scandlines.com/about-us/our-green-agenda/zero-emission-freight-ferry/> (accessed Jul. 11, 2023).
- [23] N. Murgovski, L. Johannesson, and J. Sjöberg, "Convex modeling of energy buffers in power control applications," *IFAC Proceedings Volumes*, vol. 45, no. 30, pp. 92–99, 2012, doi: 10.3182/20121023-3-FR-4025.00009.
- [24] Y. Abdul-Quadir et al., "Heat Generation in High Power Prismatic Li-Ion Battery Cell with LiMnNiCoO₂ Cathode Material," *Intl J of Energy Research*, vol. 38, no. 11, pp. 1424–1437, 2014, doi: 10.1002/er.3156.
- [25] S. Madani, E. Schaltz, and S. Knudsen Kær, "Heat Loss Measurement of Lithium Titanate Oxide Batteries under Fast Charging Conditions by Employing Isothermal Calorimeter," *Batteries*, vol. 4, no. 4, p. 59, 2018, doi: 10.3390/batteries4040059.
- [26] Z. Gao, H. Xie, X. Yang, W. Niu, S. Li, and S. Chen, "The Dilemma of C-Rate and Cycle Life for Lithium-Ion Batteries under Low Temperature Fast Charging," *Batteries*, vol. 8, no. 11, p. 234, 2022, doi: 10.3390/batteries8110234.
- [27] MAN Energy Solutions, *Batteries on board ocean-going vessels: Investigation of the potential for battery propulsion and hybridisation by the application of batteries on board*. Denmark, 2019.
- [28] M. Wetter, W. Zuo, T. S. Noudui, and X. Pang, "Modelica Buildings library," *Journal of Building Performance Simulation*, vol. 7, no. 4, pp. 253–270, 2014, doi: 10.1080/19401493.2013.765506.
- [29] C. Arpagaus, F. Bless, M. Uhlmann, J. Schiffmann, and S. S. Bertsch, "High temperature heat pumps: Market overview, state of the art, research status, refrigerants, and application potentials," *Energy*, vol. 152, pp. 985–1010, 2018, doi: 10.1016/j.energy.2018.03.166.
- [30] F. Baldi, T.-V. Nguyen, and F. Ahlgren, "The Application of Process Integration to the Optimisation of Cruise Ship Energy Systems: A Case Study," in *ECOS 2016, Portorož, Slovenia*, A. Kitanovski and A. Poredoš, Eds., 2016.
- [31] O. Konur, O. Y. Saatcioglu, S. A. Korkmaz, A. Erdogan, and C. O. Colpan, "Heat exchanger network design of an organic Rankine cycle integrated waste heat recovery system of a marine vessel using pinch point analysis," *Intl J of Energy Research*, vol. 44, no. 15, pp. 12312–12328, 2020, doi: 10.1002/er.5212.
- [32] C. Vering, "Optimal design of heat pump systems for existing buildings," *Aachen*, 2023.